A Novel Approach for Measuring Absolute Rate Constants by Pulsed Electron Spin Resonance: Addition of Phosphinoyl and 2-Hydroxy-2-propyl Radicals to Several Alkenes[†,‡]

Matthias Weber and Nicholas J. Turro*

Chemistry Department, Columbia University, 3000 Broadway, New York, New York 10027

Received: August 1, 2002; In Final Form: November 22, 2002

A time-resolved Fourier transform electron spin resonance (TR FT ESR) method for determining absolute rate constants of reactive, free radical reactions is described. The phase memory times T_M of a family of reacting radicals were measured precisely by electron spin−echo (ESE) detection. In all cases the ESE signal decays show a simple pseudo-first-order behavior. Rate constants of the reactions were extracted from the linear relationship between the reciprocal of the T_M values and the alkene concentrations. The validity of the method is demonstrated for the measurement of the rate constant for addition of different phosphinoyl and 2-hydroxy-2-propyl radicals to several acrylates, methyl methacrylate, and vinyl pivalate in organic solvents at room temperature. The results are in excellent agreement with those obtained by other kinetic investigations employing time-resolved steady-state electron spin resonance (TR CW ESR) and optical absorption spectroscopy. The technique is shown to be applicable to systems with rate constants between 10^4 and 10^8 M^{-1} s^{-1}, a range covered by the alkenes examined.

Introduction

Radical addition reactions have been an important area for research in free radical chemistry and chemical kinetics over many decades. In addition, radical addition reactions are important both in polymer chemistry and in organic synthesis; phosphorus- and carbon-centered radicals are widely used in these fields.[1−11] The reaction enthalpy of the addition step is a key factor in determining the rate of radical addition reactions. However, an interplay of steric, polar, and substituent effects, in addition to reaction enthalpy, can affect the rate constant of addition to a double bond.[6,10−16]

Radicals can be generated efficiently and under controlled conditions by photolytic α-cleavage of a suitable photoinitiator.[17−20] Upon absorption of a photon of suitable wavelength, photoinitiators undergo homolytic bond cleavage to produce two identical or two different reactive radicals. These reactive and transient radicals undergo self- and cross-termination to nonradical products or convert to other reactive radical species (e.g., by hydrogen abstraction or addition reactions, fragmentation, or rearrangements). Depending on the radical and the reaction, the rate constants of additions of radicals to a double bond may vary by many orders of magnitude.[11,21] Conventionally, for determination of the rate constants of radical reactions, one applies kinetic isolation conditions, i.e., the generation of the primary species in a short pulse and then the tracking of its conversion by a direct spectroscopic technique. In cases where direct detection is not technically convenient or possible, often competition with the formation of an indicator radical that can be directly monitored spectroscopically is employed. These conditions are often fulfilled for laser flash photolysis experiments with optical detection (UV−vis, IR) which are applied to measure high rate constants;[22−31] however, the lack of an appropriate chromophore to monitor many radical systems requires appeal to techniques involving competing kinetics relative to a known standard.[26,32−35] The competition kinetics techniques increase the complexity and sometimes the duration of the experiments, both of which are undesirable when a large number of rate constants are required.

Optical methods of radical detection, while convenient for kinetic analysis, are poor in structural information on the chromophore (responsible for absorption). On the other hand, magnetic resonance techniques can, in principle, provide rich structural information on paramagnetic species involving radical species. Recently, chemically induced dynamic nuclear polarization (CIDNP) has been used to determine absolute rate constants to several alkenes.[36] However, the CIDNP method does not provide any direct information about the structure of the reacting radicals, since only the products formed from radicals are observed.

The electron spin resonance (ESR) technique provides a powerful tool for investigating the reactivity of radicals because it not only allows direct observation of the radicals but also gives structural and dynamic information on these species and some insight in the reaction mechanism.[37−39] Different techniques have been developed in order to acquire the time profiles of the reacting radicals in obtaining absolute rate constants. For example, rate constants from 1 to 10^6 M^{-1} s^{-1} can be measured by the rotating sector technique.[40] In most cases, termination reactions, which are often close to diffusion-controlled, compete with the reaction of interest and require multiparameter fits to theoretical rate laws. A recently developed improvement in the rotating sector method[41] allows the determination of higher rate constants (10^5−10^9 M^{-1} s^{-1}). This method takes advantage of a delayed radical formation in the light-off period but affords a high signal-to-noise ratio.

Time-resolved continuous-wave ESR (TR CW ESR) detects the radical signals directly without use of the field modulation of the spectrometer and has, therefore, a higher time resolution than does the rotating sector technique (down to several hundred nanoseconds in comparison to several hundred microseconds)

[†] Part of the special issue "George S. Hammond & Michael Kasha Festschrift."

[‡] Dedicated to George S. Hammond in celebration of his 80th birthday.

* Corresponding author.

10.1021/jp021790x CCC: $25.00
Published on Web 03/19/2003

but requires strong spin polarization of the radicals to ensure suitable signal-to-noise characteristics.[42−48] The latter can be achieved by choosing photoinitiators that generate strong polarized radicals after laser flash excitation of the photoinitiator. However, the extraction of rate constants from intensity−time profiles is tedious and time-consuming. In addition, the detected signals are influenced by technical issues (*Q*-value of cavity, time constants of amplifier, homogeneity of the magnetic field, etc.), and spin polarization processes that do not directly correlate with the time evolution of the radical concentration. Therefore, polarization and relaxation parameters must be determined independently for a quantitative analysis.[49] As a result, only in rare cases has the TR CW ESR decay method been used for kinetic measurements.[50−54]

Another approach is to determine absolute rate constants from TR ESR spectra by analyzing the line width (ΔB) of the reacting radical in dependence of the quencher concentration.[35] These line widths are then converted to the effective spin−spin relaxation time T_2* with one of the following assumptions of an appropriate line shape by application of the following equations:[55]

$$\frac{1}{T_2^*} = 2\pi\nu\frac{\Delta B}{B_0} \quad \text{(Lorentzian line shape)} \qquad (1a)$$

$$\frac{1}{T_2^*} = \frac{2\pi}{\sqrt{\pi \ln 2}}\nu\frac{\Delta B}{B_0} \quad \text{(Gaussian line shape)} \qquad (1b)$$

where T_2* is the effective spin−spin relaxation time, ν is the microwave frequency, ΔB is the half-width at half-height of the ESR resonance line, and B_0 is the magnetic field at the position of the observed resonance. A linear relationship was found[35] between $1/T_2$* and the quencher concentration, given by

$$\frac{1}{T_2^*} = \frac{1}{T_{20}^*} + k[\mathrm{A}] \qquad (2)$$

where T_{20}* is the quencher-independent relaxation time, k is the rate of reaction, and [A] is the quencher concentration.

The most critical point of this method is the conversion of the measured line width to absolute time constants, because an assumption about the line shape (eqs 1a,b) must be made. This problem can be overcome by time-resolved Fourier transform ESR (TR FT ESR), which has the potential to measure T_2* relaxation times directly. Rate constants have been measured from the effective spin−spin relaxation time T_2* of the free induction decay (FID) of the ESR lines of the reacting radical as a function of the quencher concentration.[56−63] The detected FIDs can be described by a damped cosine characterized by an exponential damping rate, but even for the simplest case of the excitation of a single line by the microwave pulse at least two fit parameters are necessary. Only a few radicals fulfill this condition, which represents a strong restriction of this method. Even in the case of the simplest radical, the hydrogen atom,[56] it has been pointed out that the large covariance between the fitting parameters produces a rather scattered plot for $1/T_2$* vs the quencher concentration, unless the data were of very good quality. On the other hand, transverse relaxation times (or more exactly the phase memory time T_M, which is equal to the transverse relaxation time T_2* for homogeneous line broadening) can be measured with high precision through two-pulse electron spin−echo (ESE) techniques,[64−66] which are an exact analogue of those employed in NMR.[67,68] In this method one records the echo signal in dependence of the delay time between the two microwave pulses and analyzes the resulting decay.[69] Therefore, this method does not depend on the number of excited lines (as long as all excited lines have the same relaxation time) by the microwave pulse and make no assumption about the line shape as is necessary for the TR CW ESR techniques described above.

In this paper we measured the phase memory time T_M of transient radicals in solution with the ESE technique (two-pulse sequence), which is both simple and accurate compared to use of the FID and which allows the use of radicals other than hydrogen or deuterium atoms. The reciprocal relaxation times depend linearly on the concentration of the added scavenger (e.g., alkenes) so that absolute rate constants can be extracted from linear plots. We demonstrate the scope and effectiveness of the ESE technique (two-pulse sequence) for addition of different phosphinoyl and 2-hydroxy-2-propyl radicals to several alkenes in tetrahydrofuran (THF) and/or toluene. The radicals were produced by photolysis of the corresponding acylphosphine oxides[70−72] and α-hydroxy ketones,[17−20] which have been used for many years as photoinitiators for free radical polymerization and, therefore, were used in our studies. Some addition rate constants obtained by other techniques[26,30,31,35,36,52,73,74] have been reported in the literature. Since some of these values were measured in different solvents, they cannot be compared directly and therefore were also determined by the line width method (TR CW ESR)[35] under the same conditions as were the pulsed experiments.

Experimental Section

Materials and Solvents. The structures of the compounds employed in the production of radicals are shown in Chart 1. (2,4,6-Trimethylbenzoyl)diphenylphosphine oxide (**1**) obtained from BASF was recrystallized from diethyl ether (Aldrich). Bis-(2,6-dimethoxybenzoyl)-2,4,4-trimethylpentylphosphine oxide (**2**) and bis(2,4,6-trimethylbenzoyl)phenylphosphine oxide (**3**) (Ciba Specialty Chemicals) were recrystallized from ethanol. 2-Hydroxy-2-methyl-1-phenylpropan-1-one (**4**) (Ciba Specialty Chemicals), methyl acrylate (**5**), *n*-butyl acrylate (**6**), *tert*-butyl acrylate (**7**), vinyl acrylate (**8**), methyl methacrylate (**9**), and vinyl pivalate (**10**) (all from Aldrich) were used as received. HPLC-grade toluene from Aldrich and tetrahydrofuran (THF, inhibitor-free) from Acros were used as solvents without further purification.

Time-Resolved Fourier Transform (TR FT) ESR Experiments. Two-pulse electron spin−echo (ESE) experiments were performed on a TR FT ESR instrument that has been described earlier[75] and consists of a Bruker ESP 300/380E pulsed FT ESR spectrometer. Photochemical excitation was performed with a Quanta-Ray INDI 50−10 Nd:YAG laser (λ = 355 nm, 7 ns, 10 Hz, 10 mJ/pulse). A home-built coaxial quartz flow cell with an inner diameter of 3 mm was used in combination with a syringe pump (flow rate of 2 mL/min). Solutions of the photoinitiators (2.8−3.3 mM, absorbance at 355 nm ≈ 0.05−0.08) were prepared fresh and deoxygenated by bubbling with argon for at least 30 min. Experiments were carried out in THF or toluene at 296 ± 2 K. The spectra were recorded by a two-pulse ESE sequence (laser flash−t−90°−τ−180°−τ−echo) with t = 80 ns and τ = 96 ns (see Figure 1) in combination with an eight-phase cycling in order to suppress unwanted signals. Microwave pulse lengths of 16 ns for the first pulse (90°) and 32 ns for the second pulse (180°) were used in the experiments. The excitation range of the microwave field was around ΔB = ±0.5 mT under our experimental conditions and was less than the spectral range of the radicals (14−37 mT). Therefore, it was necessary to record the spectra of each line separately at

CHART 1: Structure of Compounds Used

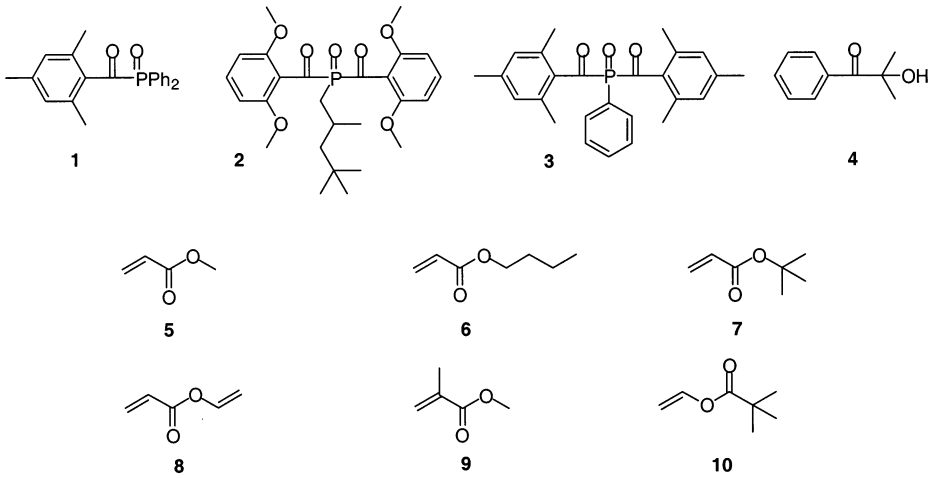

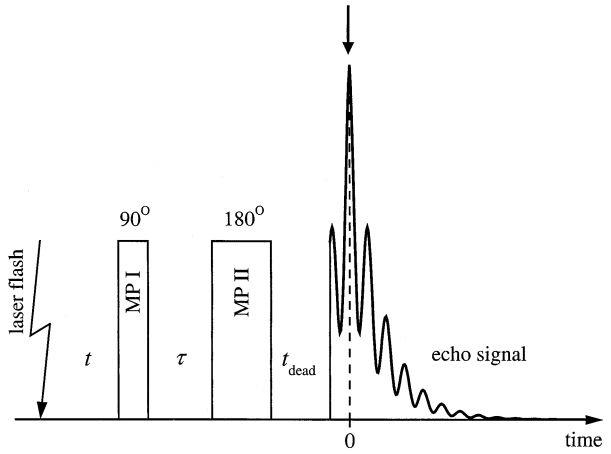

Figure 1. Schematic representation of the general pulse sequence used in this work. A single point of an echo signal not affected by the dead time (t_{dead}), as exemplified by the arrow, is used to measure the echo amplitude.

their corresponding magnetic field positions in order to measure the whole ESR spectra.

Relaxation times T_M were measured as follows. The signal intensity $S(\tau)$ at a single point of the echo signal after a two-pulse sequence (laser flash−t−90°−τ−180°−τ−echo), initiated $t = 80$ ns after the laser flash, was recorded for a series of τ values ranging from 136 to 400−2500 ns depending on the decay rate. The dwell times were set such that 50−80 points represented the decay curve. T_M was calculated from the exponential fit of the τ dependence of the echo amplitude to

$$S(\tau) = S_0 \exp\left[-\left(\frac{2\tau}{T_M}\right)^x\right] \quad (3)$$

with S_0 (initial echo amplitude), x (determined by the mechanism of phase memory time and the rate of the dephasing process relative to τ[76,77]), and T_M as fitting parameters. The echo decay in our experiments could be described by a monoexponential decay ($x \approx 1$), which is very common for dilute solutions, so that the phase memory time is equal to the spin−spin relaxation time T_2 in such cases.[78] The ESR line of the added radical with the highest intensity was chosen for kinetic analysis.

Time-Resolved Continuous-Wave (TR CW) ESR Experiments. The spectrometer was described in detail earlier[79−81] and consists of a Bruker ER 100D X-band ESR spectrometer (Bruker ESP 300 console and a Bruker ER 100D X-band magnet), an EG&G PAR boxcar integrator model 4402, and signal processor model 4402. Typically, TR ESR spectra were recorded over a period of 10 min while 512−2048 points were used. Integration over a given time window was made after the laser pulse was performed. Prior excitation was performed with a Continuum Surelite I Nd:YAG laser ($\lambda = 355$ nm, 8 ns, 30 Hz, 9 mJ/pulse), and a quartz flow cell with a 0.3 mm path length was used in combination with a syringe pump and flow rates between 1 and 3.0 mL/min. Argon-saturated solutions of the photoinitiators in THF or toluene were prepared fresh at concentrations such that the absorbance was ca. 0.3 at the excitation wavelength. All experiments were carried out at 296 ± 2 K.

Additional rate constants were determined from TR CW ESR spectra.[35] The ESR line of the reacting radical (**1a**−**4a**) is recorded in a well-defined time interval after the laser flash so that the initial broadening is nearly negligible but the signal-to-noise level is still good enough to get reasonable data. The shape of the lines was analyzed by nonlinear least-squares fitting to[55,82]

$$Y(B) = Y_{max}\frac{\Delta B^2}{\Delta B^2 + (B - B_0)^2} \quad \text{(Lorentzian line shape)} \quad (4a)$$

$$Y(B) = Y_{max}\cdot\exp\left[-\ln 2\cdot\left(\frac{B - B_0}{\Delta B}\right)^2\right] \quad \text{(Gaussian line shape)} \quad (4b)$$

where $Y(B)$ is the TR CW ESR signal intensity at the magnetic field position B, Y_{max} is the maximum signal intensity of the ESR resonance line at the magnetic field position B_0, and ΔB is the half-width at half-height. Lorentzian line shapes lead to a better fit of the experimental data compared with Gaussian line shapes if alkenes are present. The linewidth ΔB was converted to absolute relaxation times by use of eq 1a, and linear fit of eq 2 to the T_2* dependence on the alkene concentration [A] yields the additional rate constant k from the slope.

Hyperfine coupling constants (HFC) were determined by comparing simulated ESR spectra (WINEPR SimFonia, Version 1.25, Bruker Analytische Messtechnik GmbH) with the experimental data.

Result and Discussion

Absolute Addition Rate Constants of Phosphinoyl Radicals to Several Alkenes. *Reactions of Diphenylphosphinoyl Radicals*. Upon irradiation, (2,4,6-trimethylbenzoyl)diphen-

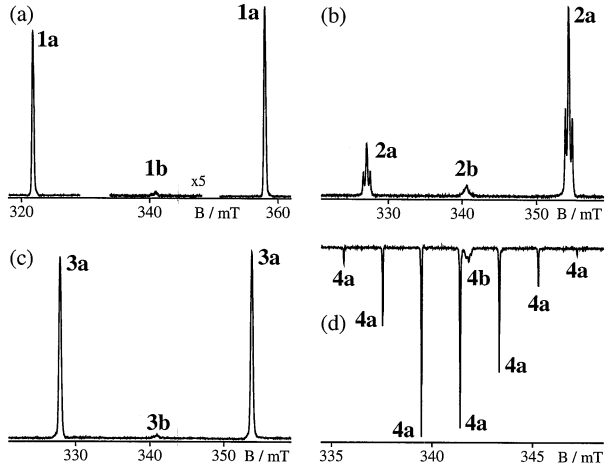

Figure 2. ESE spectra ($\tau = 96$ ns) recorded 80 ns after laser excitation of (a) **1** (2.8 mM), (b) **2** (3.3 mM), (c) **3** (3.3 mM) in toluene, and (d) **4** (2.8 mM) in THF at 296 K.

ylphosphine oxide (**1**), which is widely used as a photoinitiator for free radical polymerization,[20,83−85] undergoes fast α-cleavage from a triplet excited state to produce strongly spin-polarized diphenylphosphinoyl radicals (**1a**) and 2,4,6-trimethylbenzoyl (**1b**):[86−90]

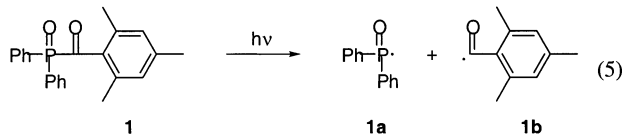

(5)

The ESE spectra recorded 80 ns after photolysis of **1** are presented in Figure 2a. Similar spectra were observed[48,74,79,87,91−93] and analyzed earlier.[92,93] The spectrum is polarized in net absorption due to the triplet mechanism[45,94−98] and shows a doublet of singlets due to the diphenylphosphinoyl radical **1a**. The observed phosphorus hyperfine coupling constant of $a(P_\alpha) = 36.2 \pm 0.1$ mT agrees with literature values.[35,74,93,99] In addition, a weak broad absorptive singlet can be observed near the centerfield and assigned to the benzoyl radicals (**1b**), whose signal intensity relative to the corresponding phosphinoyl radical is much weaker than in the well-established TR CW ESR spectra[74,79,87,91,93] due to the different detection methods. The TR CW method depends mainly on the spin−lattice relaxation time T_1, and the TR FT method depends mainly on the phase memory time T_M, and therefore, the difference found can result from the different relaxation times of the two radicals as was shown earlier for other systems.[100−102] The faster spin−spin relaxation time of the benzoyl radical **1b**, as opposed to the phosphinoyl radical **1a,** results in a much weaker signal for **1b** in the TR FT ESR spectra.

Photolysis of solutions containing **1** and alkenes **5**−**10** produces ESR spectra of radicals formed by addition of **1a** to the unsubstituted C-atom of the double bond of the alkene, as was demonstrated previously for the same or similar compounds.[73,74,93,103,104] Figure 3 shows the ESE signal intensity of the diphenylphosphinoyl radical **1a** vs time in the absence (Figure 3a) and in the presence (Figure 3b,c) of *n*-butyl acrylate **6** at different concentrations. Fits to eq 3 are superimposed over the data, and the bottom traces are fit residuals. Table 1 gives the parameters of the fits to kinetic decays for several concentrations of **6**. In all cases, the parameter x (eq 3) was nearly equal to 1 within the experimental uncertainty and therefore was set at $x = 1$ for further analysis. Analysis of the

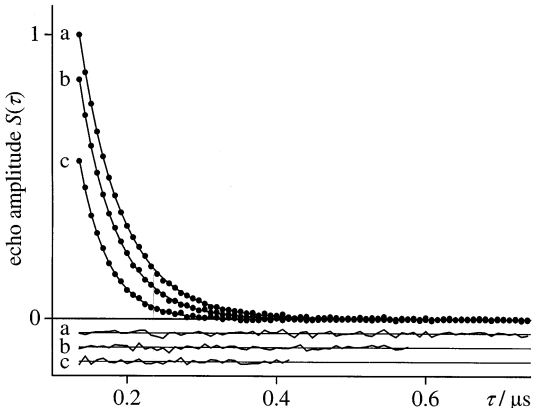

Figure 3. Relative ESE intensity (●) of the diphenylphosphinoyl radical (**1a**) vs delay time τ in toluene 80 ns after the laser flash in the presence of (a) 0 mM, (b) 70 mM, and (c) 209 mM *n*-butyl acrylate (**6**) at 296 K and fits of eq 3 (lines). Bottom traces are residuals of the fitting amplified by a factor of 2.

TABLE 1: Parameters S_0, T_M, and x Obtained by Fitting of Eq 3 to Decays of the ESE Signal Intensity of Diphenylphosphinoyl Radicals 1a in the Presence of Different *n*-Butyl Acrylate 6 Concentrations in Toluene at 296 K

[**6**], mM	S_0,[a] au	T_M,[a] ns	x[a]
0	10.41 (92)	117 (7)	1.01 (3)
70	14.1 (16)	99.8 (7)	1.05 (4)
140	22.8 (31)	85.5 (8)	1.04 (4)
209	32.5 (181)	75.8 (12)	1.05 (11)
279	51.4 (235)	67.3 (11)	1.02 (10)

[a] Standard deviations are given in parentheses in units of the last quoted digit.

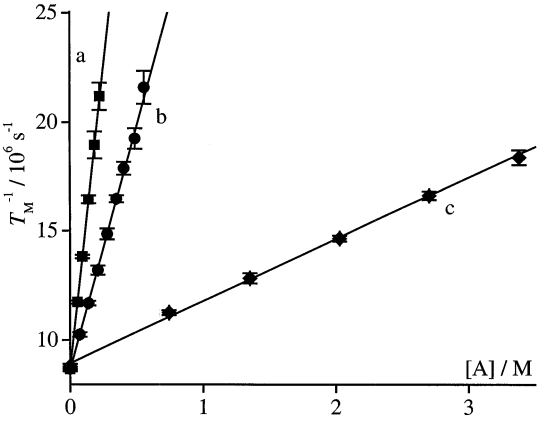

Figure 4. Pseudo-first-order plot for the addition of the diphenylphosphinoyl radical (**1a**) to (a) methyl methacrylate (**9**), (b) *n*-butyl acrylate (**6**), and (c) vinyl pivalate (**10**) in toluene at 296 K.

high-field ESR line of **1a** with eq 4b gives a line width of $\Delta B = 0.15$ mT, which corresponds, under our experimental conditions, to a spin−spin relaxation time $T_2^* = 58.3$ ns (eq 1b). This value is smaller by a factor of 2 than the determined phase memory time T_M by the ESE technique, indicating a nonhomogeneous line broadening resulting from nonresolved hyperfine couplings of the aromatic protons.[74] Plots of T_M^{-1} vs different alkene concentrations were linear (see Figure 4) and provided the rate constants k from the slope by using eq 2. Table 2 summarizes the absolute rate constants for the reaction of **1a** to several acrylates and vinyl pivalate at room temperature in toluene measured by the concentration dependence of the phase memory time T_M. It was shown previously[35] that absolute rate

TABLE 2: Absolute Rate Constants for the Addition of Diphenylphoshinoyl Radicals 1a to Several Alkenes in Toluene at 296 K Determined by TR FT and TR CW ESR

	k,[a] 10^7 M^{-1} s^{-1}	
alkene	TR FT ESR	TR CW ESR
methyl acrylate (**5**)	2.33 (6)	2.04 (10)
n-butyl acrylate (**6**)	2.27 (4)	2.04 (10)
tert-butyl acrylate (**7**)	2.34 (2)	2.09 (8)
vinyl acrylate (**8**)	3.39 (10)	3.34 (15)
methyl methacrylate (**9**)	5.55 (3)	5.34 (29)
vinyl pivalate (**10**)	0.274 (5)	0.203 (6)

[a] Standard deviations are given in parentheses in units of the last quoted digit.

constants for these reactions can be measured by the newlyintroduced line width method with TR CW ESR detection. Because of the lack of absolute rate constants for the addition of **1a** to the set of alkenes used in our study in toluene under our conditions, we determined these rate constants also by using this new method (spectra were recorded between 300 and 400 ns), which are also given in Table 2.

The TR FT method yields the same rate constants k within the experimental uncertainties, but they are systematically slightly lower than the values from the TR CW ESR experiments. The origins of these systematic deviations are probably artifacts resulting from methods used and not the chemical systems, which were the same for both techniques. Because of the more direct ESE technique, the phase memory time can be measured much more precisely than by analyzing the ESR line shape, which requires additional assumptions about the line shape and, therefore, may cause the observable systematic errors. The rate constants for the addition of **1a** to *n*-butyl acrylate in toluene were found to be $k = (1.79 \pm 0.07) \times 10^7$ M^{-1} s^{-1} by the TR CW method[35] and $k = (1.98 \pm 0.06) \times 10^7$ M^{-1} s^{-1} by laser flash photolysis (LFP) in combination with optical detection of **1a,** which has a strong absorption around 330 nm.[25] Other LFP measurements gave $k = 2.8 \times 10^7$ M^{-1} s^{-1} in acetonitrile[30] and $k = (2.21 \pm 0.10) \times 10^7$ M^{-1} s^{-1} in ethyl acetate[74] for the same reaction. Furthermore, the rate constants for the addition of **1a** to several alkenes were studied by LFP: $k = (3.3 \pm 0.2) \times 10^7$ M^{-1} s^{-1} in hexane to methyl acrylate,[73] $k = (3.3 \pm 0.1) \times 10^7$ M^{-1} s^{-1} in ethyl acetate to vinyl acrylate,[74] $k = (11 \pm 2) \times 10^7$ M^{-1} s^{-1} in hexane to methyl methacrylate,[73] and $k = (0.200 \pm 0.010) \times 10^7$ M^{-1} s^{-1} in ethyl acetate to vinyl pivalate.[74] Measurements by analysis of the decay of the spin polarization in TR CW ESR[52] gave rate constants for the addition of **1a** in benzene to methyl methacrylate of $k = (1.6 \pm 0.4) \times 10^7$ M^{-1} s^{-1} and to vinyl pivalate of $k = (0.25 \pm 0.01) \times 10^7$ M^{-1} s^{-1}. All literature values are in good agreement with our results (except k for methyl methacrylate[52,73]), indicating the applicability of our method to measure absolute rate constant by use of the electron spin−echo technique.

Reactions of Acylphosphinoyl Radicals. We extended our kinetic studies to measure the rate constants for the addition of two acylphosphinoyl radicals to *n*-butyl acrylate in order to test the reported technique for radicals, whose rate constants were determined earlier by different methods.[30,35] The photochemistry and photophysics of bis(acyl)phosphine oxides (**2** and **3**) are similar to those of the mono(acyl)phosphine oxides (**1**) and are fairly well understood.[30,79,86−90] After excitation with light, photoinitiators **2** and **3** undergo an efficient α-cleavage from the excited triplet state to produce strongly spin-polarized

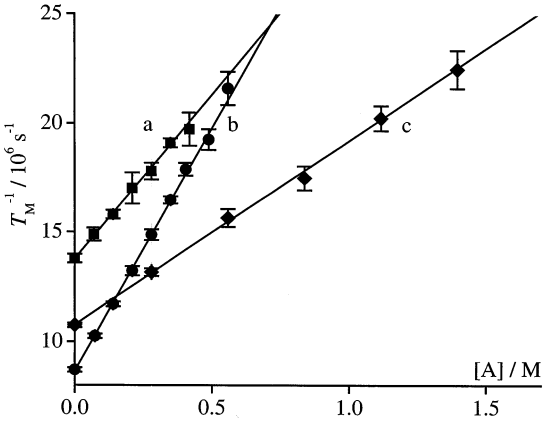

Figure 5. Pseudo-first-order plot for the addition of (a) **2a**, (b) **1a**, and (c) **3a** to *n*-butyl acrylate (**6**) in toluene at 296 K.

acylphosphinoyl (**2a**, **3a**) and benzoyl (**2b**, **3b**) radicals:

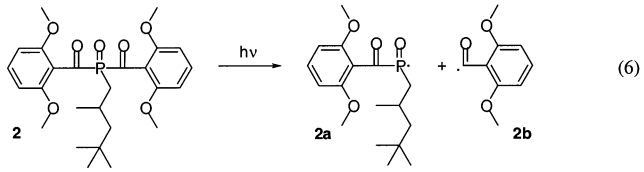

(6)

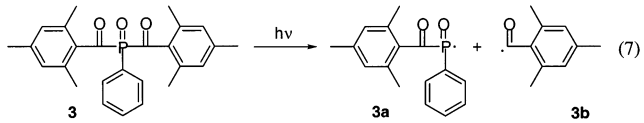

(7)

The resulting ESE spectra recorded 80 ns after photolysis are presented in Figure 2b,c and are in agreement with the literature.[30,35] The spectra show the well-known absorptive doublet of triplets (**2a**) or singlets (**3a**) signals of the phosphinoyl and weak broad absorptive singlets of the benzoyl radicals (**2b** and **3b**) near the centerfield. Phase memory times of $T_M = 70.7 \pm 0.7$ ns for **2a** and $T_M = 96.4 \pm 0.5$ ns for **3a** were determined in the absence of alkenes, which are slightly lower than those for the diphenylphosphinoyl radical **1a**. Figure 5 shows a plot of T_M^{-1} for the radicals **1a**−**3a** vs the *n*-butyl acrylate concentration. Absolute addition constants k yield from the slope of the linear regression of eq 2 to the data and were determined to be $k = (1.42 \pm 0.04) \times 10^7$ M^{-1} s^{-1} for **2a** and $k = (0.839 \pm 0.16) \times 10^7$ M^{-1} s^{-1} for **3a**. Good agreement was found in comparison with rate constants obtained by the line width method[35] to $k = (1.14 \pm 0.15) \times 10^7$ M^{-1} s^{-1} for **2a** and $k = (0.765 \pm 0.022) \times 10^7$ M^{-1} s^{-1} for **3a** and by optical detection to $k = 1.5 \times 10^7$ M^{-1} s^{-1} [30] and $k = (1.41 \pm 0.12) \times 10^7$ M^{-1} s^{-1} [35] for **2a** and $k = 1.1 \times 10^7$ M^{-1} s^{-1} [30] and $k = (0.867 \pm 0.019) \times 10^7$ M^{-1} s^{-1} [35] for **3a**.

Absolute Addition Rate Constants of 2-Hydroxy-2-propyl Radicals to Several Alkenes. α-Hydroxy ketones, such as 2-hydroxy-2-methyl-1-phenylpropanone (**4**), have been used for many years as photoinitiators for free radical polymerization.[17−20] Photolysis of **4** (2.8 mM) in THF produces a dimethyl ketyl−benzoyl radical pair **4a** and **4b** (eq 8) after a fast type I cleavage[105,106] with a triplet lifetime of $\tau_T = 0.37$ ns.[107]

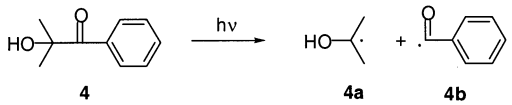

(8)

The significant academic and industrial interest in α-hydroxy ketones comes from the high reactivity of **4a** toward alkenes,

which is an important step in free radical polymerization. Consequently, factors controlling the rate constants have been the subject of much experimental and theoretical work.[11,26,85,108,109] Unfortunately, the radical **4a** has a low extinction coefficient at wavelengths higher than 300 nm[26] and therefore is very difficult to detect directly by laser flash photolysis employing optical methods. In addition, overlapping optical absorptions of the initiator molecule (**4**), the 2-hydroxy-2-propyl (**4a**) and the benzoyl (**4b**) radicals complicate the kinetic analysis with optical detection methods. Absolute rate constants were measured by introducing a competing kinetic process that produces a radical with an appropriate chromophore and with a known rate constant.[26,31] Despite these technical difficulties, a few rate constants were determined directly by the optical detection method of **4a** by use of a symmetric precursor (2,4-dihydroxy-2,4-dimethylpentan-3-one).[26]

Other methods, such as the rotating sector technique in combination with CW ESR,[109] are restricted to rate constants up to 10^6 M^{-1} s^{-1}, and the analysis of TR ESR decays are complicated by polarization processes. The TR FT ESR method offers for radicals such as **4a** a method to measure directly absolute rate constants with a high precision, as we will demonstrate in the following paragraph.

Figure 2d presents the ESE ESR spectrum of **4** (2.8 mM) in THF recorded 80 ns after laser flash photolysis, which agrees with similar time-resolved ESR spectra observed earlier.[48,74,107,110] The septet of doublets of the 2-hydroxy-2-propyl (dimethyl ketyl) radicals **4a** are emissively polarized by the triplet mechanism as reported earlier[74,110] with coupling constants of $a(6H_\beta) = 1.933 \pm 0.005$ mT [$a(6H_\beta) = 1.93-1.98$ mT[111]] and $a(OH) = 0.022 \pm 0.002$ mT [$a(OH) = 0.03-0.07$ mT[111]]. A weak broad emissive singlet can be detected near the centerline of radical **4a** that corresponds to the benzoyl radicals (**4b**) with a slightly lower *g*-factor ($\bar{g} = 2.0007$[111,112]) than the 2-hydroxy-2-propyl radical ($\bar{g} = 2.0031$[111,112]). Similar to the other photoinitiators **1**−**3,** the signal intensity ratio of the benzoyl **4b** to **4a** is much lower than in the TR CW ESR spectra[48,74,107,110] due to the different relaxation times of these radicals. In the absence of alkenes, the phase memory T_M of the benzoyl radical **4b** was determined to be $T_M = 142 \pm 4$ ns in THF and $T_M = 139 \pm 8$ ns in toluene, whereas the dimethyl ketyl radicals **4a** have higher values by a factor of 6 of $T_M = 890 \pm 50$ ns in THF and $T_M = 800 \pm 35$ ns in toluene. No phase memory times for the benzoyl radical were found in the literature, but good agreement was found for **4a** with the reported values measured in 2-propanol of $T_2 = 850 \pm 100$ ns[113] by modulated ESR and ≈1000 ns[114] by analysis of the FID of the perdeuterated radical **4a** from TR FT ESR experiments; however, Tominaga et al.[115] determined a higher spin−spin relaxation rate of 2700 ns from the decay of TR CW ESR signal by assuming $T_1 = T_2$.

In the presence of alkenes **5**−**10**, dimethyl ketyl radicals add to the unsubstituted carbon atom of the alkene as was shown previously for the same or similar compounds.[26,31,48,54,74,102,109] Figure 6 shows the ESE signal intensity of the 2-hydroxy-2-propyl radical **4a** against the delay time τ for different concentrations of *n*-butyl acrylate in THF at room temperature. Fits of eq 3 to the decays yielded the phase memory times T_M. Similar to the phosphinoyl radicals **1a**−**3a**, the values *x* were around 1, indicating a monoexponential decay, and therefore, *x* was set to 1 for further analysis. Plots of T_M^{-1} vs alkene concentrations were linear (Figure 7), and linear regression of eq 2 to the data yielded the absolute addition constant *k* from the slope. Table 3 summarizes the absolute rate constants for

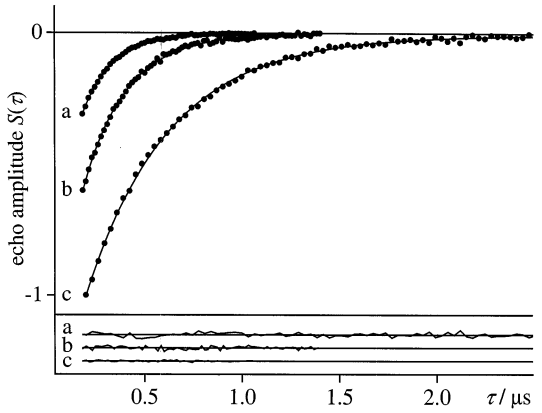

Figure 6. Relative ESE intensity (●) of the 2-hydroxy-2-propyl radical (**4a**) vs delay time τ in THF 80 ns after the laser flash in the presence of (a) 0 mM, (b) 56 mM, and (c) 111 mM *n*-butyl acrylate (**6**) at 296 K and fitting of eq 3 (lines). Bottom traces are residuals of the fitting amplified by a factor of 2.

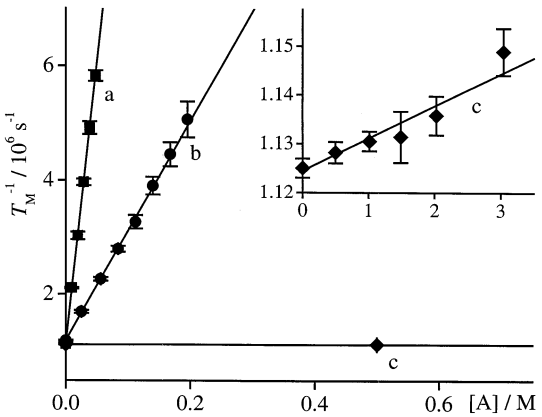

Figure 7. Pseudo-first-order plot for the addition of the 2-hydroxy-2-propyl radical (**4a**) to (a) vinyl acrylate (**8**), (b) *n*-butyl acrylate (**6**), and (c) vinyl pivalate (**10**) in THF at 296 K. The inset shows in more detail the pseudo-first-order plot for vinyl pivalate.

TABLE 3: Absolute Rate Constants for the Addition of 2-Hydroxy-2-Propyl Radicals 1d to Several Alkenes in Toluene and Tetrahydrofuran (THF) at 296 K Determined by TR FT and TR CW ESR

	k,[a] 10^7 M^{-1} s^{-1}		
alkene	TR FT ESR (THF)	TR FT ESR (toluene)	TR CW ESR (toluene)
methyl acrylate (**5**)	2.17 (3)	1.80 (11)	1.72 (6)
n-butyl acrylate (**6**)	1.96 (3)	1.65 (8)	1.96 (8)
tert-butyl acrylate (**7**)	1.70 (10)	1.19 (3)	1.11 (5)
vinyl acrylate (**8**)	9.75 (3)	5.78 (13)	5.55 (19)
methyl methacrylate (**9**)	0.617 (9)	0.541 (22)	0.534 (34)
vinyl pivalate (**10**)	0.00066 (25)	0.0005 (3)	< 0.03[b]

[a] Standard deviations are given in parentheses in units of the last quoted digit. [b] Rate constant lower than sensitivity of the method.

the addition of **4a** to the alkenes **5**−**10** at room temperature in THF and toluene. It can be seen from this table that the addition rate constants in THF are higher by a factor of up to 1.7 compared to those in toluene, which is in agreement with earlier results of the solvent dependence.[36]

It was reported earlier,[26,31,36,109] that the rate constants for the addition of 2-hydroxy-2-propyl radicals to alkenes vary by over 8 orders of magnitude with alkene substitution and show strong polar solvent effects of up to 1 order of magnitude. A direct comparison with our results is difficult, because the absolute rates from the literature were determined for different

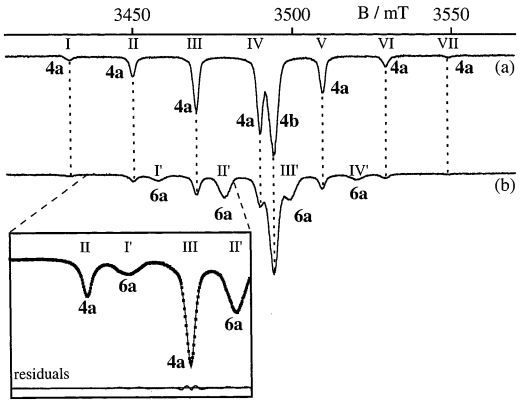

Figure 8. TR CW ESR spectra recorded 100−200 ns following laser excitation of **4** (2.8 mM) in toluene solution at 296 K in the (a) absence of alkenes and (b) presence of 391 mM *n*-butyl acrylate (**6**). The inset shows a part of spectrum b and a fitting of eq 10 (line) to the data (■) together with the resulting residuals.

alkenes and/or in different solvents, and therefore, we repeated the measurements for the addition of **4a** to the same set of alkenes **5**−**10** in toluene by using the well-established line width method with TR CW ESR detection.[35] In contrast to radicals **1a**−**3a**, with their huge phosphorus coupling constants of a couple of tens of millitesla, which are extending the spectral range of the adduct radicals,[73,74,93] the dimethyl ketyl **4a** has a much smaller one of $a(6H_\beta) = 1.933 \pm 0.005$ mT, resulting in an interference of its ESR spectrum with the resonance lines of the adduct radicals resulting from the addition of **4a** to the double bond (for examples see refs 48, 54, 74, 102, and 116). The overlapping of ESR lines complicates the line width analysis. The TR CW ESR spectrum recorded 100−200 ns after photolysis of **4** in toluene is presented in Figure 8a. It shows the emissive seven lines of **4a** and a strong broad signal near the centerfield corresponding to **4b**, which is much more pronounced than in the TR FT ESR spectrum (Figure 2d) as mentioned above. The line width of the 2-hydroxy-2-propyl radical **4a** is higher than in the TR FT ESR spectrum (Figure 2d) as a result of unresolved hyperfine coupling of the hydrogen of the OH group and loss of the second-order splittings.[54,74,113,117,118] The lower resolution of the TR CW method was observed earlier for similar systems[100,102,118] and is caused mainly by the detection method at these early delay times (e.g., response time of the amplifier, high *Q*-value of the cavity). The addition of 2-hydroxy-2-propyl **4a** radicals to *n*-butyl acrylate **6** produces adduct radicals **6a**.[31,54,102]

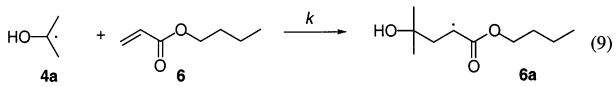

(9)

The emissive polarization is transferred to the adduct radicals by addition of **4a** to the alkenes (**5**−**10**);[31,54,74,110] the adducts produced also show net E-pattern of polarization. Figure 8b shows the TR CW ESR recorded 100−200 ns after the laser flash of **4** in the presence of *n*-butyl acrylate **6** in toluene at 296 K. The benzoyl (**4b**) has much lower reactivity than the dimethyl ketyl (**4a**) indicated by the nearly unchanged signal intensity in the TR CW ESR spectra.[54,74,110] The additional ESR lines in the presence of **6** correspond to the adduct radical **6a** with coupling constants of $a(1H_\alpha) \approx a(2H_\beta) = 2.05$ mT, in agreement with earlier reported values.[54,102]

The line width of the 2-hydroxy-2-propyl radical **4a** decreases for longer delay times, but in contrast to the phosphinoyl radicals **1a**−**3a**,[35] no constant width could be observed even after 2 μs

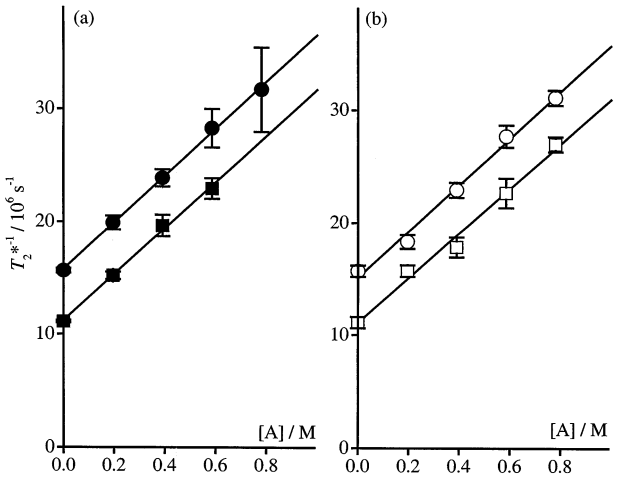

Figure 9. Pseudo-first-order plot for the addition of 2-hydroxy-2-propyl radical (**4a)** to *n*-butyl acrylate (**6**) in toluene at 296 K determined by the line width method with delay times of 100−200 ns (circles) and 300−400 ns (squares) by analyzing (a) line group II (closed symbols) and (b) line group III (open symbols).

of detection. Therefore, we recorded TR CW ESR spectra a couple of hundred nanoseconds after the laser flash for the determination of rate constants by the line width method,[35] accepting some line broadening by the spectrometer but taking advantage of a better signal-to-noise ratio for the 2-hydroxy-2-propyl radical **4a** and less signal from the resulting adduct radical **6a** (whose polarization is building up on this time scale). The first two low-field lines of **4a** (line groups II and III; see Figure 8) were used for the kinetic measurements (centerline IV is overlapping with the benzoyl radical **4b**, the outer line groups I and VII are too weak in intensity, and the line groups V and VI are weaker in intensity than those used). In this region two lines (I′ and II′) of the adduct radical **6a** overlap with the two lines (groups II and III) of **4a**, and therefore this part of the spectrum must be analyzed with four Lorentzian line shapes simultaneously given by

$$Y(B) = \sum_{i=1}^{4} Y_{\max,i} \frac{\Delta B_i^2}{\Delta B_i^2 + (B - B_{0,i})^2} \qquad (10)$$

where $Y(B)$ is the TR CW ESR signal intensity at the magnetic field position B, $Y_{\max,i}$ is the maximum signal intensity of the ESR resonance line i at the magnetic field position $B_{0,i}$, and ΔB_i is the half-width at half-height for the ESR line i. The analysis requires at least 12 independent fit parameters (three parameters $Y_{\max,i}$, ΔB_i, and $B_{0,i}$ for each line) and therefore affords a high signal-to-noise ratio. The inset of Figure 8 shows the line groups II, III, I′, and II′ of the TR CW ESR recorded 100−200 ns after the laser flash of **4** in the presence of *n*-butyl acrylate **6** in toluene at 296 K, together with the fit to eq 10 to the spectra and the resulting residuals. To exclude instrumental artifacts, we determined the rate constants using the line groups II and III of the added radical **4a** with delay times of 100−200 ns and 300−400 ns. Figure 9 shows plots of T_2^{*-1} vs alkene concentrations [A] after converting the determined line widths to absolute relaxation times by using eq 1a. In all cases the experimental data show a linear behavior and we got the same rate constant k for the addition of **4a** to *n*-butyl acrylate **6** within the experimental uncertainties from the slope by linear regression of eq 2 to the data [line group II, k(100−200 ns) = (2.14 ± 0.22) × 10^7 M^{-1} s^{-1} and k(300−400 ns) = (2.05 ± 0.08) × 10^7 M^{-1} s^{-1}; line group III, k(100−200 ns) = (1.96 ± 0.08) ×

10^7 M^{-1} s^{-1} and $k(300-400\ ns) = (1.91 \pm 0.12) \times 10^7$ M^{-1} s^{-1}]. The results demonstrate the independence of the selected delay times and analyzed line group. These rate constants are similar to the values determined by the TR FT ESR method for this reaction and are in acceptable agreement with the literature where different solvents and/or acrylates were used [k(**6**) = (2.28 $\pm$ 0.34) $\times$ 10^7 M^{-1} s^{-1} in toluene;[119] k(**6**) = 1.3 $\times$ 10^7 M^{-1} s^{-1} in acetonitrile;[31] k(**5**) = 3.5 $\times$ 10^7 M^{-1} s^{-1} in methanol;[26] k(**5**) = 1.3 $\times$ 10^7 M^{-1} s^{-1} in acetonitrile;[31] k(**5**) = 0.65 $\times$ 10^7 M^{-1} s^{-1} in toluene-d_8[36]]. The onset values are smaller for the delay times of 300−400 ns (T_{20}* = 91 $\pm$ 5 ns) than for 100−200 ns (T_{20}* = 64 $\pm$ 1 ns) but are still lower than the phase memory time for **4a** in toluene (T_M = 800 $\pm$ 35 ns) measured by TR FT EPR. In the following experiments we used delay times of 100−200 ns and the line group III to measure the absolute rate constants k for the addition of the 2-hydroxy-2-propyl radical (**4a**) to the alkenes **5**−**10** in toluene at 296 K while giving the best signal-to-noise ratio. Table 3 compares these absolute addition rate constants with the results determined by the TR FT ESR technique and demonstrates that the two experimental techniques yield k in good agreement with each other. Again, higher rate constants were determined by using the TR FT ESR method as it was observed previously for the diphenylphosphinoyl radical **1a** (see above).

Conclusion

TR FT ESR spectroscopy is a suitable tool to measure the phase memory time of transient radicals with high reproducibility and accuracy by a two-pulse sequence (ESE technique). Absolute rate constants were determined from the concentration dependence of the phase memory time for the addition of radicals **1a**−**4a** to several alkenes **5**−**10** that are in good agreement with the literature and the values obtained by the ESR line width analysis. TR FT ESR has several advantages compared to TR CW, such as a higher precision, lower influence by instrumental artifacts, and the use of lower alkene concentrations (less influence of viscosity changes). The method presented allows the determination of absolute rate constants over several orders of magnitude up to the diffusion-controlled region (10^9 M^{-1} s^{-1}) and can be used in cases where optical experiments fail due to insufficient resolution, sensitivity, or other technical reasons. Furthermore, ESR provides direct detailed structural information of the reactive species and the transformed radicals and, therefore, gave an insight to the reaction mechanism.

Acknowledgment. We thank the National Science Foundation (CHE98-12676 and CHE01-10655) for generous support of this research. This work was supported in part by the MRSEC Program of the National Science Foundation under Award DMR-02-13574. Professor David Doetschman (SUNY Binghamton) is thanked for informative discussions about pulsed ESR and the electron spin echo technique.

References and Notes

(1) Rüchardt, C. *Angew. Chem., Int. Ed. Engl.* **1970**, *9*, 830.
(2) Tedder, J. M.; Walton, J. C. *Tetrahedron* **1980**, *36*, 701.
(3) Beckwith, A. L. J. *Tetrahedron* **1981**, *37*, 3073.
(4) Tedder, J. M. *Angew. Chem., Int. Ed. Engl.* **1982**, *21*, 401.
(5) Giese, B. *Angew. Chem., Int. Ed. Engl.* **1983**, *22*, 753.
(6) Giese, B. *Angew. Chem., Int. Ed. Engl.* **1989**, *28*, 969.
(7) Motherwell, W. B.; Crich, D. *Free Radical Chain Reactions in Organic Synthesis*; Academic Press: London, 1992.
(8) Moad, G.; Solomon, D. H. *The Chemistry of Free Radical Polymerization*; Elsevier Science: Oxford, U.K., 1995.
(9) Fossey, J.; Lefort, D.; Sorba, J. *Free Radicals in Organic Chemistry*; John Wiley & Sons: New York, 1995.
(10) Fischer, H.; Minisci, F., Eds. Kluwer Academic Publishers: Dordrecht, The Netherlands, 1997; pp 63−74.
(11) Fischer, H.; Radom, L. *Angew. Chem., Int. Ed.* **2001**, *40*, 1340.
(12) Walling, C. *Free Radicals in Solution*; John Wiley & Sons: New York, 1957.
(13) Pryor, W. A. *Introduction to Free Radical Chemistry*; Prentice Hall: Englewood Cliffs, NJ, 1966.
(14) Tedder, J. M.; Walton, J. C. *Acc. Chem. Res.* **1976**, *9*, 183.
(15) Tedder, J. M.; Walton, J. C. *Adv. Phys. Org. Chem.* **1978**, *18*, 51.
(16) Tedder, J. M. *Angew. Chem.* **1982**, *94*, 433.
(17) Eichler, J.; Herz, C. P. *Farbe Lack* **1979**, *85*, 933.
(18) Herz, C. P.; Eichler, J.; Neisius, K. H. *Kontakte (E. Merk)* **1979**, 31.
(19) Dietliker, K. *Photoinitiators for Free Radical and Cationic Polymerization*; SITA Technology Ltd.: London, 1991; Vol. 3.
(20) Dietliker, K. In *Radiation Curing in Polymer Science and Technology*; Fouassier, J. P., Rabek, J. F., Eds.; Elsevier Applied Science: New York, 1993; Vol. II, p 155.
(21) Landolt-Börnstein *Radical Reaction Rates in Liquids*; New Series, Springer: Berlin, 1983−1997; Vol. II/13, II/18.
(22) Scaiano, J. C. *Acc. Chem. Res.* **1983**, *16*, 234.
(23) Neville, A. G.; Brown, C. E.; Rayner, D. M.; Lusztyk, J.; Ingold, K. U. *J. Am. Chem. Soc.* **1989**, *111*, 9269.
(24) Tsentalovich, Y. P.; Fischer, H. *J. Chem. Soc., Perkin Trans. 2* **1994**, 729.
(25) Sluggett, G. W.; Turro, C.; George, M. W.; Koptyug, I. V.; Turro, N. J. *J. Am. Chem. Soc.* **1995**, *117*, 5148.
(26) Martschke, R.; Farley, R.; Fischer, H. *Helv. Chim. Acta* **1997**, *80*, 1363.
(27) Wagner, B. D.; Ruel, G.; Lusztyk, J. *J. Am. Chem. Soc.* **1996**, *118*, 13.
(28) Nau, W. M.; Cozens, F. L.; Scaiano, J. C. *J. Am. Chem. Soc.* **1996**, *118*, 2275.
(29) Jockusch, S.; Timpe, H.-J.; Schnabel, W.; Turro, N. J. *J. Phys. Chem. A* **1997**, *101*, 440.
(30) Jockusch, S.; Turro, N. J. *J. Am. Chem. Soc.* **1998**, *120*, 11773.
(31) Jockusch, S.; Turro, N. J. *J. Am. Chem. Soc.* **1999**, *121*, 3921.
(32) Avila, D. V.; Ingold, K. U.; Lusztyk, J.; Dolbier, W. R.; Pan, H.-Q. *J. Am. Chem. Soc.* **1993**, *115*, 1577.
(33) Avila, D. V.; Ingold, K. U.; Lusztyk, J.; Dolbier, W. R.; Pan, H.-Q. *J. Am. Chem. Soc.* **1994**, *116*, 99.
(34) Rong, X. X.; Pan, H.-Q.; Dolbier, W. R.; Smart, B. E. *J. Am. Chem. Soc.* **1994**, *116*, 4521.
(35) Gatlik, I.; Rzadek, P.; Gescheidt, G.; Rist, G.; Hellrung, B.; Wirz, J.; Dietliker, K.; Hug, G.; Kunz, M.; Wolf, J.-P. *J. Am. Chem. Soc.* **1999**, *121*, 8332.
(36) Batchelor, S. N.; Fischer, H. *J. Phys. Chem.* **1996**, *100*, 9794.
(37) Hore, P. H.; Joslin, C. G.; McLauchlan, K. A. In *Chemically Induced Dynamic Electron Polarization in Electron Spin Resonance*; Specialist Periodical Reports, No. 5; The Chemical Society: Burlington House: London, 1979; p 1.
(38) Hirota, N.; Yamauchi, S. In *Studies in Physical and theoretical Chemistry*; Kuchitsu, K., Ed.; Elsevier: Amsterdam, 1994; Vol. 82, p 513.
(39) Forbes, D. E. *Photochem. Photobiol.* **1997**, *65*, 73.
(40) Fischer, H.; Paul, H. *Acc. Chem. Res.* **1987**, *20*, 200.
(41) Weber, M.; Fischer, H. *J. Am. Chem. Soc.* **1999**, *121*, 7381.
(42) Muus, L. T.; Atkins, P. W.; McLauchlan, K. A.; Pedersen, J. B. *Chemically Induced Magnetic Polarization*; Reidel: Dordrecht, The Netherlands, 1977.
(43) McLauchlan, K. A. In *Modern Pulsed and Continuous-Wave Electron Spin Resonance*; Kevan, L., Bowman, M. K., Eds.; John Wiley & Sons: New York, 1990; pp 285−363.
(44) Forbes, M. D. E. *Spectrum* **1995**, *8*, 1.
(45) Clancy, C. M. R.; Tarasov, V. F.; Forbes, D. E. *Electron Paramagn. Reson.* **1998**, *16*, 50.
(46) Turro, N. J.; Khudyakov, I. V. *Res. Chem. Intermed.* **1999**, *25*, 505.
(47) van Willigen, H. *Mol. Supramol.* **2000**, *6*, 197.
(48) Turro, N. J.; Kleinman, M. H.; Karatekin, E. *Angew. Chem., Int. Ed.* **2000**, *39*, 4436.
(49) Savitsky, A. N.; Paul, H. *Appl. Magn. Reson.* **1997**, *12*, 449.
(50) Fessenden, R. W.; Verma, N. C. *Faraday Discuss. Chem. Soc.* **1977**, *63*, 104.
(51) Beckert, D.; Mehler, K. *Ber. Bunsen-Ges. Phys. Chem.* **1983**, *87*, 587.
(52) Kajiwara, A.; Konishi, Y.; Morishima, Y.; Schnabel, W.; Kuwata, K.; Kamachi, M. *Macromolecules* **1993**, *26*, 1656.
(53) Ohara, K.; Hirota, N.; Steren, C. A.; van Willigen, H. *J. Phys. Chem.* **1996**, *100*, 3070.
(54) Vacek, K.; Geimer, J.; Beckert, D.; Mehnert, R. *J. Chem. Soc., Perkin Trans. 2* **1999**, 2469.
(55) Ayscough, P. B. *Electron Spin Resonance in Chemistry*; Methuen & Co. Ltd.: London, 1967.

(56) Han, P.; Bartels, D. M. *Chem. Phys. Lett.* **1989**, *159*, 538.
(57) Han, P.; Bartels, D. M. *J. Phys. Chem.* **1990**, *94*, 7294.
(58) Roduner, E.; Bartels, D. M. *Ber. Bunsen-Ges. Phys. Chem.* **1992**, *96*, 1037.
(59) Bartels, D. M.; Mezyk, S. P. *J. Phys. Chem.* **1993**, *97*, 4101.
(60) Mezyk, S. P.; Bartels, D. M. *J. Phys. Chem. A* **1997**, *101*, 1329.
(61) Geimer, J.; Beckert, D.; Jenichen, A. *Chem. Phys. Lett.* **1997**, *280*, 353.
(62) Lossack, A. M.; Roduner, E.; Bartels, D. M. *Chem. Phys. Lett.* **2001**, *342*, 524.
(63) Lossack, A. M.; Roduner, E.; Bartels, D. M. *Phys. Chem. Chem. Phys.* **2001**, *3*, 2031.
(64) Forster, M. J. *J. Magn. Reson.* **1988**, *84*, 580.
(65) Keijzers, C. P.; Reijerse, E. J.; Schmidt, J. *Pulsed EPR: A new field of applications*; North-Holland: New York, 1989.
(66) Bertini, I.; Martini, G.; Luchinat, C. In *Handbook of Electron Spin Resonance*; Poole, J., C. P., Farach, H. A., Eds.; AIP Press: New York, 1994.
(67) Carr, H. Y.; Purcell, E. M. *Phys. Rev.* **1954**, *94*, 630.
(68) Cosgrove, T. *J. Magn. Reson.* **1976**, *21*, 469.
(69) Stillman, A. E.; Schwartz, R. N. *J. Phys. Chem.* **1981**, *85*, 3031.
(70) Rist, G.; Boerer, A.; Dietliker, K.; Desobry, V.; Fouassier, J. P.; Ruhlmann, D. *Macromolecules* **1992**, *25*, 4182.
(71) Rutsch, W.; Dietliker, K.; Leppard, D.; Köhler, M.; Misev, L.; Kolczak, U.; Rist, G. *Prog. Org. Coat.* **1996**, *27*, 227.
(72) Khudyakov, I. V.; Legg, J. C.; Purvis, M. B.; Overton, B. J. *Ind. Eng. Chem. Res.* **1999**, *38*, 3353.
(73) Sluggett, G. W.; McGarry, P. F.; Koptyug, I. V.; Turro, N. J. *J. Am. Chem. Soc.* **1996**, *118*, 7367.
(74) Weber, M.; Turro, N. J. *J. Phys. Chem. A* **2002**, 1938.
(75) Koptyug, I. V.; Bossmann, S. H.; Turro, N. J. *J. Am. Chem. Soc.* **1995**, *118*, 1435.
(76) Brown, I. M. In *Time Domain Electron Spin Resonance*; Kevan, L., Schwartz, R. N., Eds.; John Wiley & Sons: New York, 1979; p 195.
(77) Salihov, K. M.; Tsvetkov, Y. D. In *Time Domain Electron Spin Resonance*; Kevan, L., Schwartz, R. N., Eds.; John Wiley & Sons: New York, 1979; p 230.
(78) Norris, J. R.; Thurnauer, M. C.; Bowman, M. K. *Adv. Biol. Med. Phys.* **1980**, *17*, 365.
(79) Turro, N. J.; Khudyakov, I. V. *Chem. Phys. Lett.* **1992**, *193*, 546.
(80) Lipson, M.; McGarry, P. F.; Koptyug, I. V.; Staab, H. A.; Turro, N. J.; Doetschman, D. C. *J. Phys. Chem.* **1994**, *98*, 7504.
(81) Koptyug, I. V.; Ghatlia, N. D.; Slugglett, G. W.; Turro, N. J.; Ganapathy, S.; Bentrude, W. G. *J. Am. Chem. Soc.* **1995**, *117*, 9486.
(82) Weil, J. A.; Bolton, J. R.; Wertz, J. E. *Electron Paramagnetic Resonance*; John Wiley & Sons: New York, 1994.
(83) Jacobi, M.; Henne, A. *J. Radiat. Curing* **1983**, *10*, 16.
(84) Jacobi, M.; Henne, A. *Polym. Paint Colour J.* **1985**, *175*, 636.
(85) Schnabel, W. In *Laser in Polymer Science and Technology: Applications*; Fouassier, J. P., Rabek, J. F., Eds.; CRC Press: Boca Raton, FL, 1993; Vol. 2, p 95.
(86) Sumiyoshi, T.; Schnabel, W.; Henne, A.; Lechtken, P. *Polymer* **1985**, *26*, 141.
(87) Baxter, J. E.; Davidson, R. S.; Hageman, H. J.; McLauchlan, K. A.; Stevensen, D. G. *J. Chem. Soc., Chem. Commun.* **1987**, 73.
(88) Kolczak, U.; Rist, G.; Dietliker, K.; Wirz, J. *J. Am. Chem. Soc.* **1996**, *118*, 6477.
(89) Jockusch, S.; Koptyug, I. V.; McGarry, P. F.; Sluggett, G. W.; Turro, N. J.; Watkins, D. M. *J. Am. Chem. Soc.* **1997**, *119*, 11495.
(90) Spichty, M.; Turro, N. J.; Günther, R.; Birbaum, J.-L.; Dietliker, K.; Wolf, J.-P.; Gescheidt, G. *J. Photochem. Photobiol. A* **2001**, *142*, 209.
(91) Kamachi, M.; Kuwata, K.; Sumiyoshi, T.; Schnabel, W. *J. Chem. Soc., Perkin Trans. 2* **1988**, 961.
(92) Tarasov, V. F.; Yashiro, H.; Maeda, K.; Azumi, T.; Shkrob, I. A. *Chem. Phys.* **1998**, *226*, 253.
(93) Williams, R. M.; Khudyakov, I. V.; Purvis, M. B.; Overton, B. J.; Turro, N. J. *J. Phys. Chem. B* **2000**, *104*, 10437.
(94) Kaptein, P. W.; Oosterhoff, J. L. *Chem. Phys. Lett.* **1969**, *4*, 195.
(95) Kaptein, P. W.; Oosterhoff, J. L. *Chem. Phys. Lett.* **1969**, *4*, 214.
(96) Adrian, F. J. *J. Chem. Phys.* **1974**, *61*, 4875.
(97) Salikhov, K. M.; Molin, Y. N.; Sagdeev, R. Z.; Buchachenko, A. L. *Spin Polarization and Magnetic Field Effects in Radical Reactions*; Elsevier: Amsterdam, 1984.
(98) Wan, J. K. S.; Depew, M. C. *Res. Chem. Intermed.* **1992**, *18*, 227.
(99) Roberts, B. P.; Singh, K. *J. Org. Chem.* **1978**, *43*, 31.
(100) Iwaizumi, M.; Yamamoto, K.; Ohba, Y.; Yamauchi, S. *Coord. Chem. Rev.* **1994**, *132*, 29.
(101) Turro, N. J.; Koptyug, I. V.; Vanwilligen, H.; McLauchlan, K. A. *J. Magn. Reson., Ser. A* **1994**, *109*, 121−123.
(102) Weber, M.; Beckert, D.; Turro, N. J. *Phys. Chem. Chem. Phys.* **2002**, *4*, 168.
(103) Kamachi, M.; Kajiwara, A.; Saegusa, K.; Morishima, Y. *Macromolecules* **1993**, *26*, 7369.
(104) Mizuta, Y.; Morishita, N.; Kuwata, K. *Chem. Lett.* **1999**, 311.
(105) Eichler, J.; Herz, C. P.; Naito, I.; Schnabel, W. *J. Photochem.* **1980**, *12*, 225.
(106) Eichler, J.; Herz, C. P.; Schnabel, W. *Angew. Makromol. Chem.* **1980**, *91*, 39.
(107) Jockusch, S.; Landis, M. S.; Freiermuth, B.; Turro, N. J. *Macromolecules* **2001**, *34*, 1619.
(108) Salmassi, A.; Eichler, J.; Herz, C. P.; Schnabel, W. *Polym. Photochem.* **1982**, *2*, 209.
(109) Héberger, K.; Fischer, H. *Int. J. Chem. Kinet.* **1993**, *25*, 913.
(110) Karatekin, E.; O'Shaughnessy, B.; Turro, N. J. *Macromolecules* **1998**, *31*, 7992.
(111) Landolt-Börnstein *Magnetic Properties of Free Radicals*; New Series, Springer: Berlin, 1977; Vol. II/9b.
(112) Landolt-Börnstein *Magnetic Properties of Free Radicals*; New Series, Springer: Berlin, 1987; Vol. II/17b.
(113) Paul, H. *Chem. Phys.* **1979**, *40*, 265.
(114) Levstein, P. R.; van Willigen, H. *J. Chem. Phys.* **1991**, *95*, 900.
(115) Tominaga, K.; Yamauchi, S.; Hirota, N. *J. Chem. Phys.* **1990**, *92*, 5175.
(116) Beckert, A.; Naumov, S.; Mehnert, R.; Beckert, D. *J. Chem. Soc., Perkin Trans. 2* **1999**, 1075.
(117) Levstein, P. R.; van Willigen, H. *Zeitschr. Phys. Chem.* **1993**, *180*, 33, and references therein.
(118) van Willigen, H.; Levstein, P. R.; Ebersole, M. H. *Chem. Rev.* **1993**, *93*, 173.
(119) Gescheidt, G. Private communication.